Supplementary Information

Enhanced selectivity and mass activity for electrocatalytic reduction of CO_2 to CO on an anodized Zn/carbon/Ag electrode

Yugang Gao,[a] Fengping Li,[b] Peng Zhou,[a] Zeyan Wang,[a,*] Zhaoke Zheng,[a] Peng Wang,[a] Yuanyuan Liu,[a] Ying Dai,[b] Myung-Hwan Whangbo,[a,c,d] Baibiao Huang[a,*]

[a] State Key Laboratory of Crystal Materials, Shandong University, Jinan 250100, China

[b] School of Physics, Shandong University, Jinan 250100, China

[c] Department of Chemistry, North Carolina State University, Raleigh, North Carolina 27695-8204, USA

[d] State Key Laboratory of Structural Chemistry, Fujian Institute of Research on the Structure of Matter (FJIRSM), Chinese Academy of Sciences (CAS), Fuzhou 350002, China

Corresponding authors:

Email: wangzeyan@sdu.edu.cn, bbhuang@sdu.edu.cn

S1. Preparation of the AZ electrode

The AZ electrode, i.e., anodized Zn, was prepared in a two-electrode system using H_2O (10mL)/ethanol (40mL) solution of 0.08 M salicylic acid under the bias of 30 V for an hour with Zn foils as the anode and cathode, as illustrated **Figure S2**. A sheet of very thin Zn plates (nearly perpendicular to the Zn foil) grows on the Zn anode as the oxidation reaction proceeds (**Figure S3**).

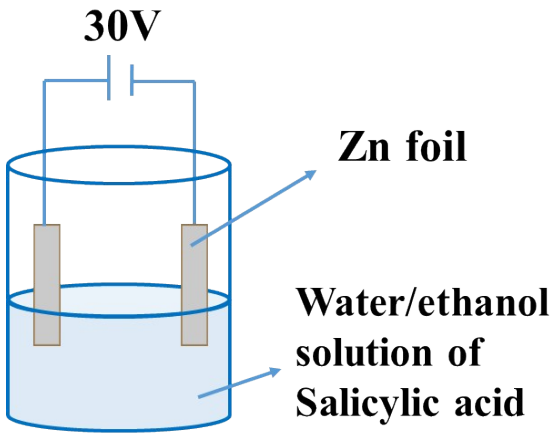

Figure S1. Preparation of the AZ electrode.

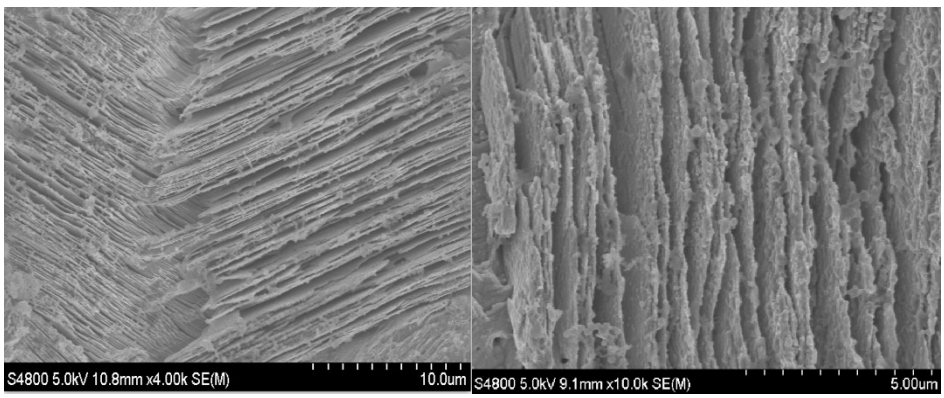

Figure S2. SEM images of the as-prepared AZ electrode in different magnification.

The as-prepared AZ electrode was washed with deionized water and then with ethanol, and was dried in a vacuum oven before using. The AZ foil (0.22 cm^2 in area) was coated with 20 μL of the C/Ag ink to form the AZ/C/Ag electrode. The sides of the AZ and AZ/C/Ag electrodes are sealed by insulant (epoxy resin).

S2. Synthesis of GCE/C/Ag electrode

Ag NPs were prepared using the chemical reduction methods.[1] 50 μL of 0.05 M silver nitrate solution, 0.5 mL of 75 mM trisodium citrate solution, and 60 μL of 30 wt% H_2O_2 were added into a 24.75mL of H_2O at room temperature. This solution, after adding 250 μL of 100 mM sodium borohydride $NaBH_4$, was stirred vigorously to obtain Ag NPs dispersed in the solution. The Ag NPs were collected from 7 mL of this solution containing Ag NPs by centrifugation several times. The mass concentration C_m of the Ag NPs contained in the 7 mL solution (see **Table S1**) was calculated as 10.75 mg/L. The amount *m* of Ag NPs in the C/Ag mixture is then given by $m = C_m \times V$, where V = 7 mL.

0.075 mg of Ag NPs (namely, the amount contained in the 7 mL solution described in the previous section) and 15 mg of C are added in a solution consisting of 200 μL water, 700 μL iso-propanol and 100 μL of 5% nafion solution. This solution was ultrasonicated for more than 5 h to form a homogenous C/Ag mixture. The carbon used in this work is carbon black, acetylene, 100% compressed. The Raman spectra of the carbon used in this work were also shown as **Figure S3**. The glassy carbon electrode (GCE) of 5 mm in diameter and AZ of 0.22 cm^{-2} was coated with 20 μL of the C/Ag mixture to form the GCE/C/Ag electrode and

AZ/C/Ag electrode, respectively.

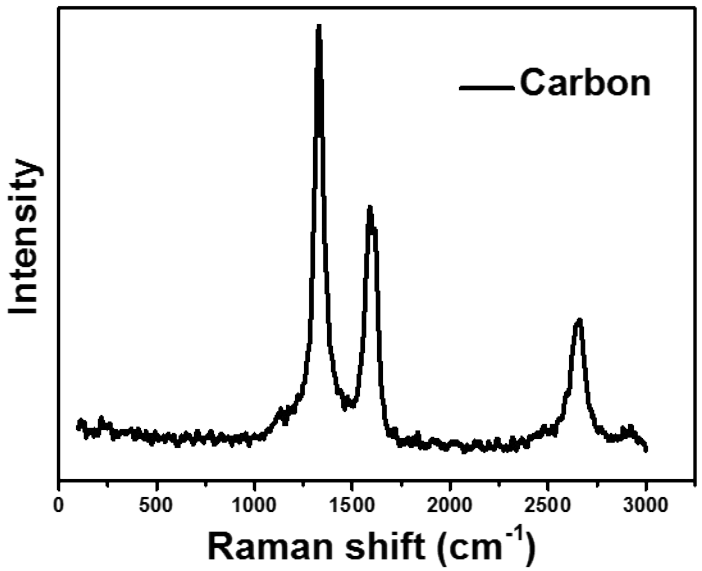

Figure S3 Raman pattern of the Carbon.

S3. Characterization

The morphologies of the electrode were examined by a field emission scanning electron microscopy (FESEM) (S-4800, Hitachi) (as seen in **Figure S4**) at a 5 kV acceleration voltage. Energy-Dispersive X-ray Spectroscopy (EDS) mapping was carried out to show the atom distribution of the three electrodes (**Figure S4**). STEM-EDS mapping images are shown in **Figure S5**. EDS pattern of the AZ/C/Ag is shown in **Figure S6**. The relative amounts of the atoms were summarized in **Table S1**.

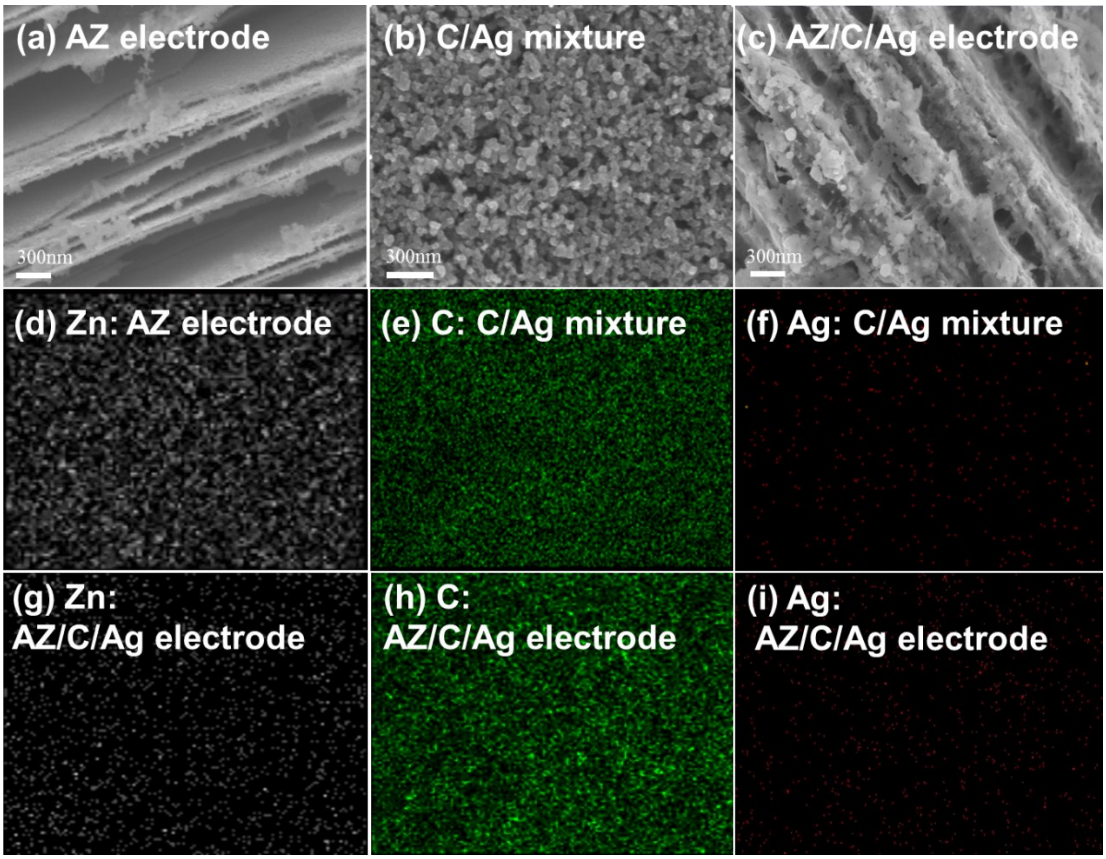

Figure S4. SEM images of (a) the AZ electrode, (b) the C/Ag mixture, (c) the AZ/C/Ag electrode. EDS mapping of the (d) Zn atoms in the AZ electrode as well as the (e) C and (f) Ag atoms in the C/Ag mixture, respectively. EDS mapping of the (g) Zn, (h) C, and (i) Ag atoms in the AZ/C/Ag electrode.

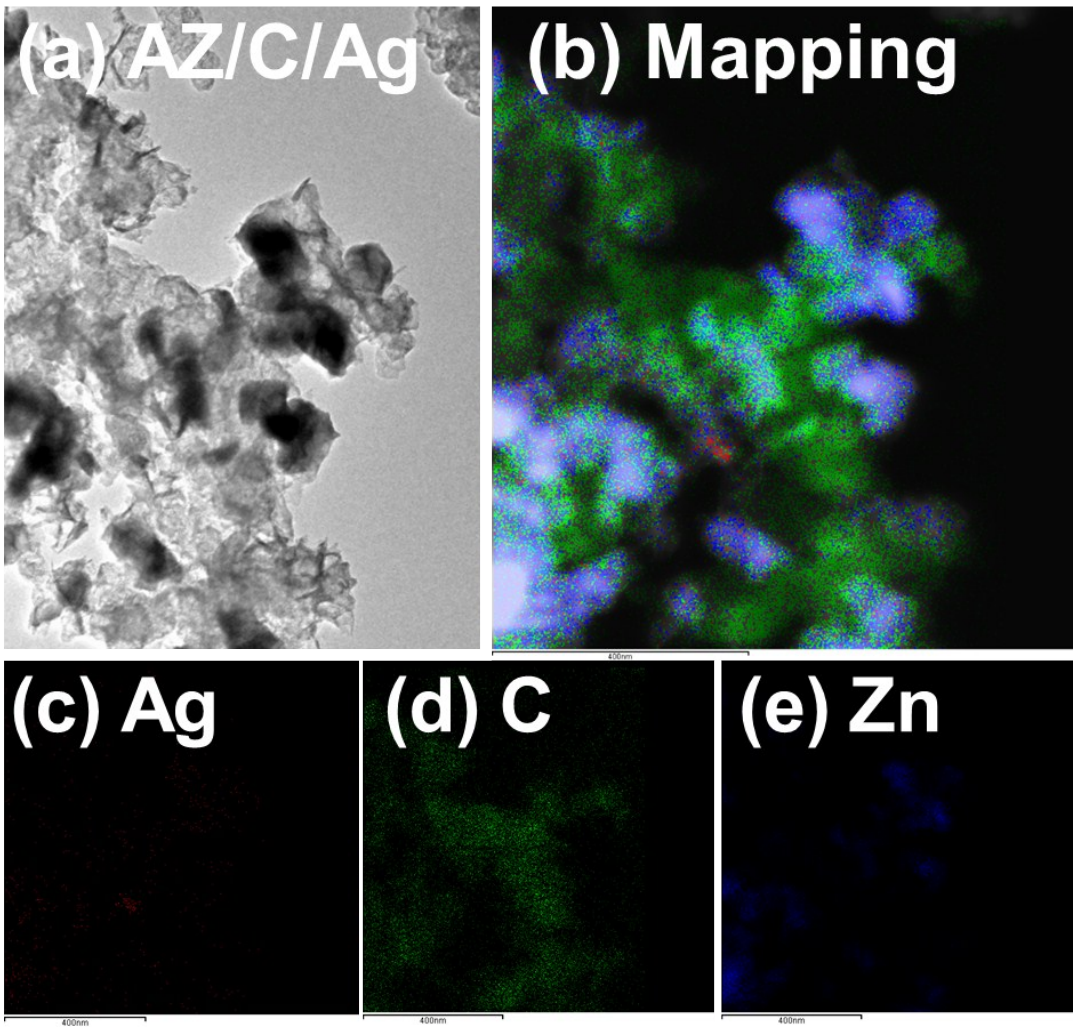

Figure S5 (a) TEM image of AZ/C/Ag nanoparticles scraped from the electrode (b) STEM image and the corresponding EDS elemental mappings of the (c) Ag atoms (d) C atoms (e) Zn atoms.

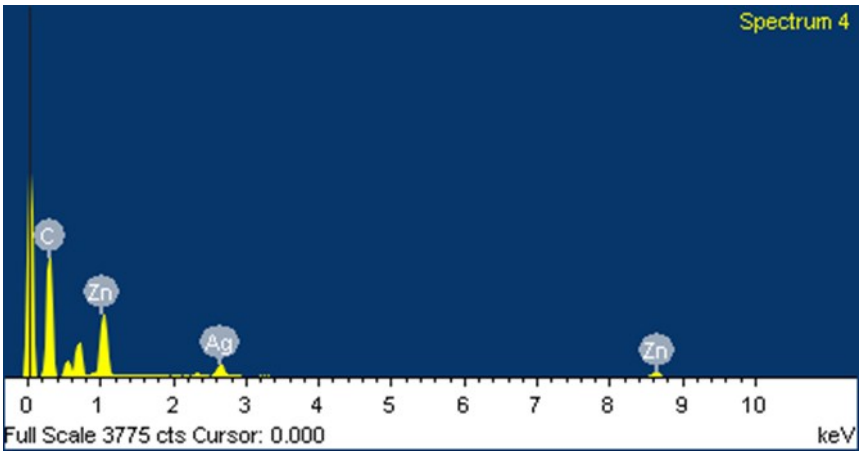

Figure S6. EDS pattern of the AZ/C/Ag electrode.

Table S1. Relative amounts of the atoms C, Zn and Ag in the AZ/C/Ag electrode deduced from the EDS measurements.

Element	Weight%	Atomic%
C K	75.60	94.39
Zn L	24.58	5.64
Ag L	-0.18	-0.02
Totals	100.00	

The crystal structure of the AZ electrode is examined by XRD (D8ADVANCE, Bruker) recorded on a Bruker AXS D8 diffractometer using Cu Kα radiation as presented in **Figure S7**.

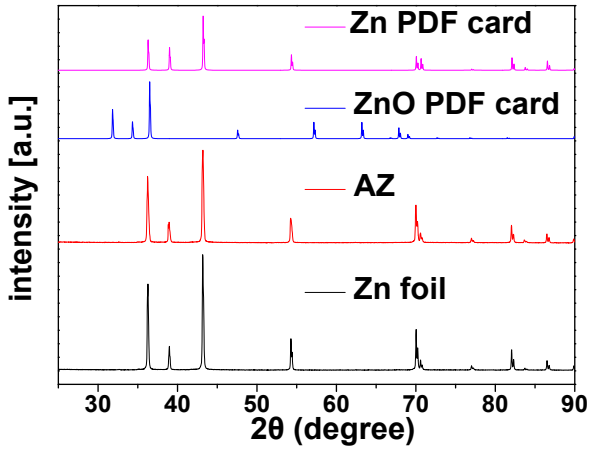

Figure S7. XRD patterns of the AZ and Zn foil electrodes.

The fine morphologies of the AZ, Ag NPs, and C/Ag NPs are examined by the transmission electron microscopy (TEM, JEOL-2100F) using a Philips Tecnai 20U-Twin microscope at an acceleration voltage of 200 kV as shown in **Figure S8** and **S9**.

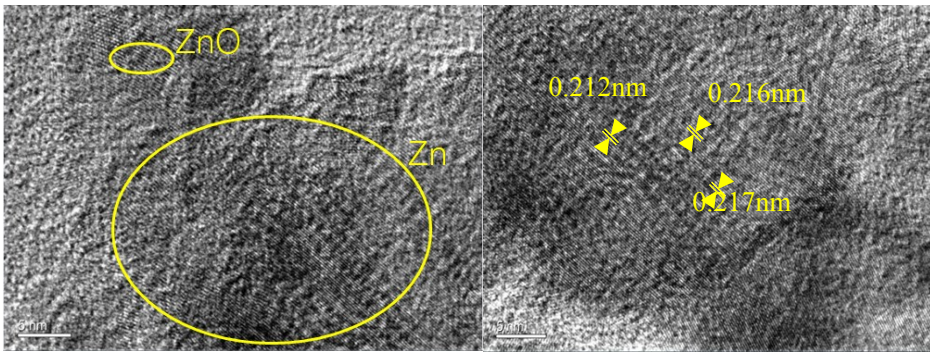

Figure S8. TEM images of the as-prepared AZ electrode

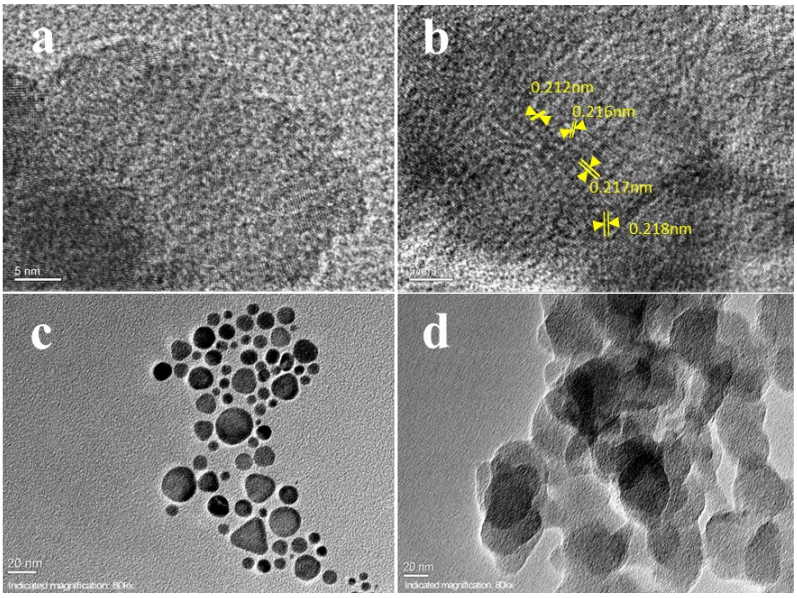

Figure S9. TEM images of the (a) AZ powders scrapped from the as-prepared AZ electrode, (c) Ag NPs and (d) C/Ag NPs, and the lattice fingers of the AZ powders.

The UV-vis adsorption spectrum of the solution containing dispersed Ag NPs, examined using Shimadzu UV 2600 spectrophotometer equipped with a cell holder, is shown in **Figure S10**. It shows a relatively sharp absorption peak centered around 400 nm, indicating that the Ag NPs are almost spherical shape as confirmed by the TEM image in **Figure S9c**.

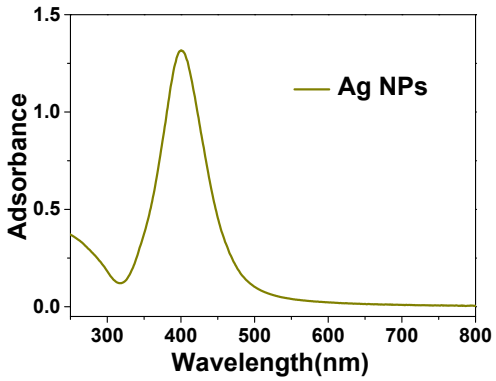

Figure S10. UV/vis spectrum of the solution with dispersed Ag NPs.

S4. RHE calibration

The RHE calibration is performed under the practical condition according to the previous reports (Figure S10).[2, 3] The calibration was carried out in the high purity hydrogen and CO_2 saturated $KHCO_3$ electrolyte with a Pt wire as the working electrode. Cycle Voltammetry was run at a scan rate of 1 mV s-1. The average of the two potentials at which the current crossed zero was taken to be the thermodynamic potential for the hydrogen electrode reactions. So in CO_2 saturated 0.5M $KHCO_3$, E (RHE) = E (Ag/AgCl) + 0.657 V.

CO_2 saturated 0.5M $KHCO_3$

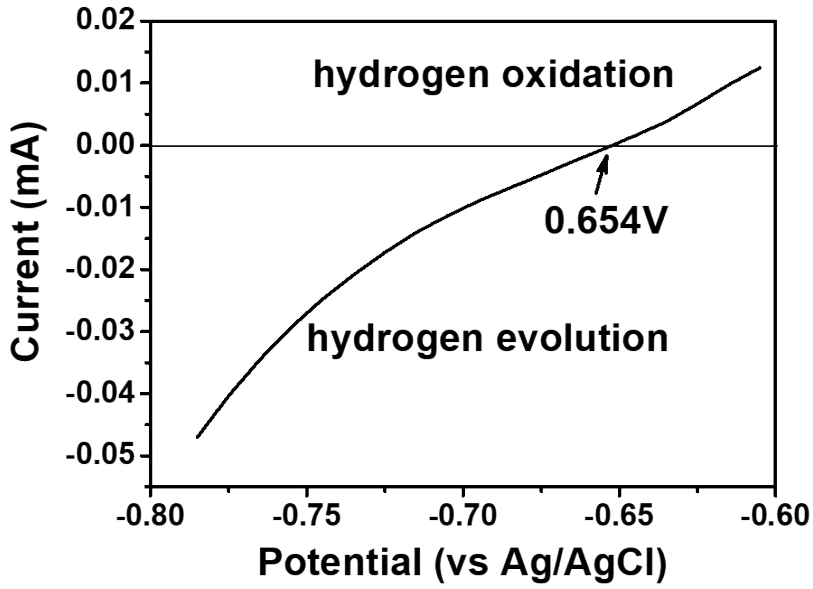

Figure S11. Calibration of Ag/AgCl reference electrode relative to the RHE.

S5. Electrochemical measurements

All electrochemical experiments were carried out using the electrochemical workstation CHI660E. The LSV measurements were performed with an Ag/AgCl reference electrode (with

saturated KCl as the filling solution), a platinum electrode as the counter electrode and the three samples (i.e., AZ, GCE/C/Ag, and AZ/C/Ag) as the working electrode. The electrolyte was potassium bicarbonate saturated with CO_2 by bubbling high-purity CO_2 gas, before each experiment, at a flow rate of 50 ml min^{-1} for 1 h to remove all oxygen from the electrolyte. The working electrode was tested 20 times before the plot is recorded at a scan rate of 50 mV s^{-1}. All potentials were transformed to the reversible hydrogen electrode (RHE) reference by using the relationship, $E_{RHE} = E_{Ag/AgCl}$ +0.654V (measured under the practical condition).

Product analysis was performed in a two-compartment electrochemical cell with an anion exchange membrane separating the working and counter electrodes. The potentiostatic measurements were performed to obtain the value of the consumed coulomb.

The gas products from the cathode compartment were examined with a gas chromatograph (GC) equipped with a TDX-01 column with a flame ionization detector (FID) and a H_2-detection GC (ShiweipxGC-7806) with a thermal conductivity detector (TCD). Gas chromatograph-mass spectrometer (GCMS) was used to determine the concentration of liquid products with a Max capillary column.

The surface roughness factor of the prepared electrodes was estimated by an electric double layer capacitance measurements.[4] Cyclic voltammetry measurements were performed on the electrodes at various scan rates (10, 20, 40, 60, 80, and 100 mV s^{-1}) in an Ar-bubbled 1 M $NaSO_4$ electrolyte between -0.72 and -0.54V vs RHE, as shown in **Figure S7**.

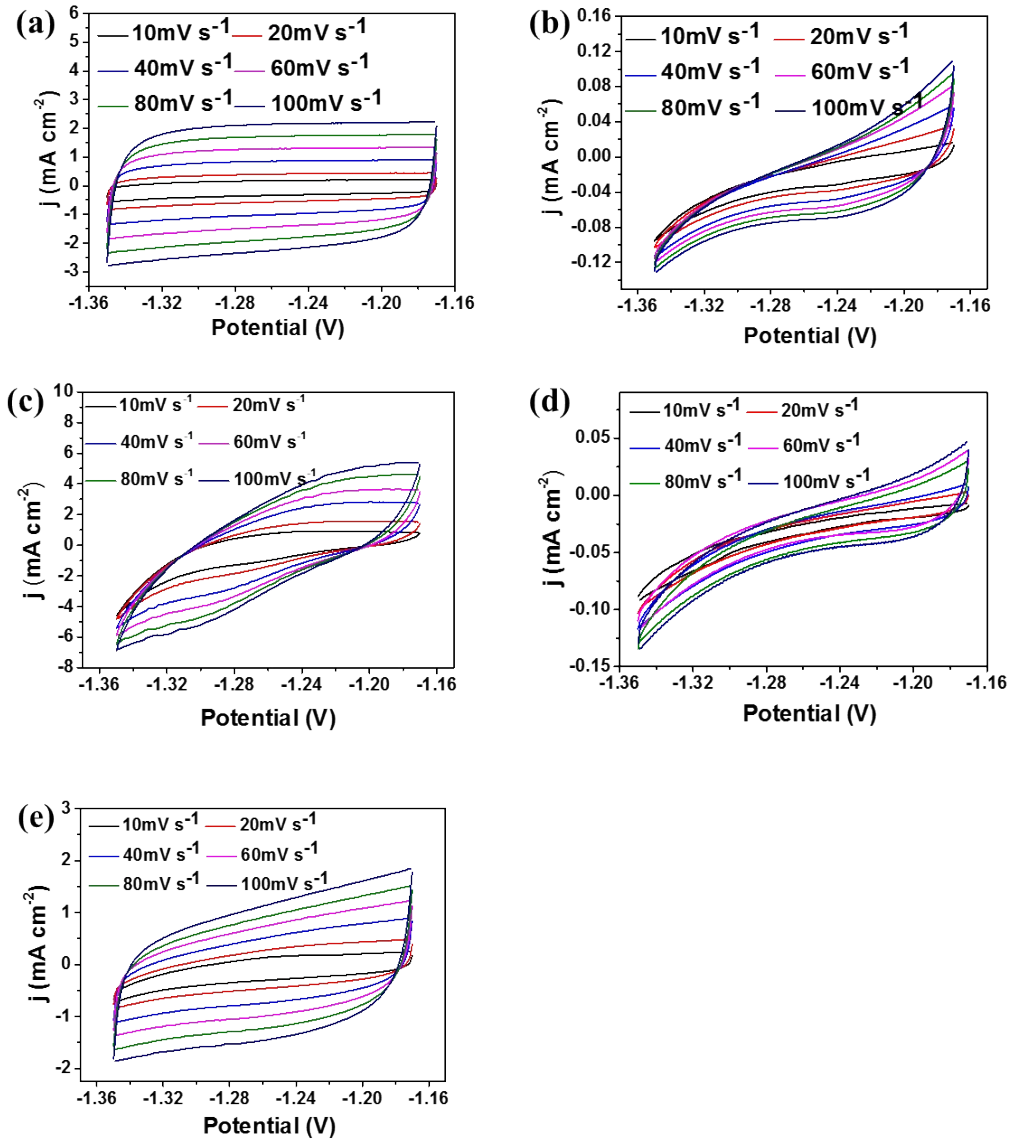

Figure S12. Cyclic voltammetry measurements for (a) the GCE/C/Ag electrode, (b) the Zn foil, (c) the AZ/C/Ag electrode, (d) the AZ electrode and (e) the AZ/C electrode.

The ECSAs (**Table S2**) of the electrodes can be determined by the following equation,

$$j = C \times dV/dt$$

$$R_f = \frac{C_{sample}}{C_{smooth}}$$

$$ECSA = R_f S$$

where j is the current density (mA cm^{-2}), C is the capacitance (mF cm^{-2}), and dV/dt (V s^{-1}) is the scan rate. S is the specific area of the smooth metal electrode.

Table S2. Values of R_f and ECSA of various electrodes

	R_f	ECSA (cm^2)
Zn foil	1	0.25
AZ/C	19.425	4.856
AZ/C/Ag	75.133	18.78
GCE	1	0.0707
GCE/C/Ag	101.875	7.203

The faradaic efficiency (FE) was calculated by the following equation

$$FE_{CO} = \frac{\alpha nF}{Q} = \frac{2nF}{It}$$

Where α is the number of the electrons transferred for CO, F is the Faraday constant, Q is the charge, *I* is the current, t is the running time and n is the total amount of CO (in moles).

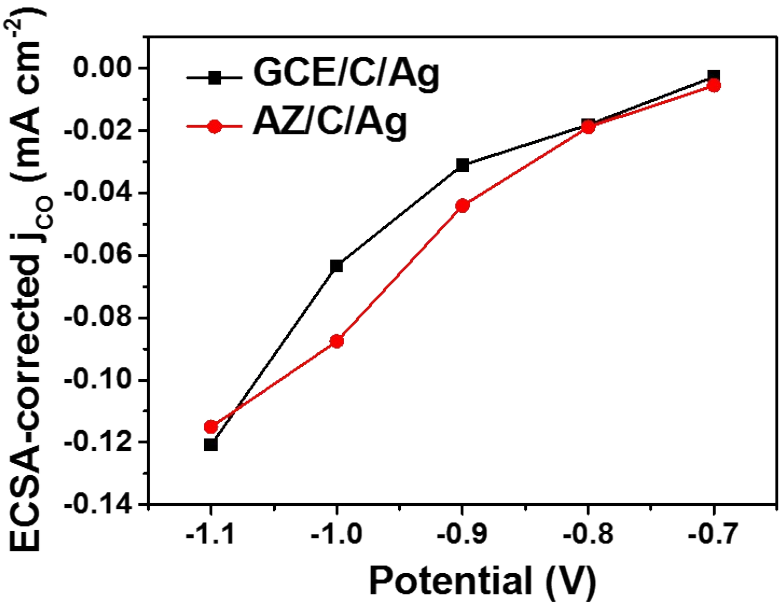

Figure S13. Current densities normalized by electrochemically active surface area for AZ/C/Ag and GCE/C/Ag electrodes.

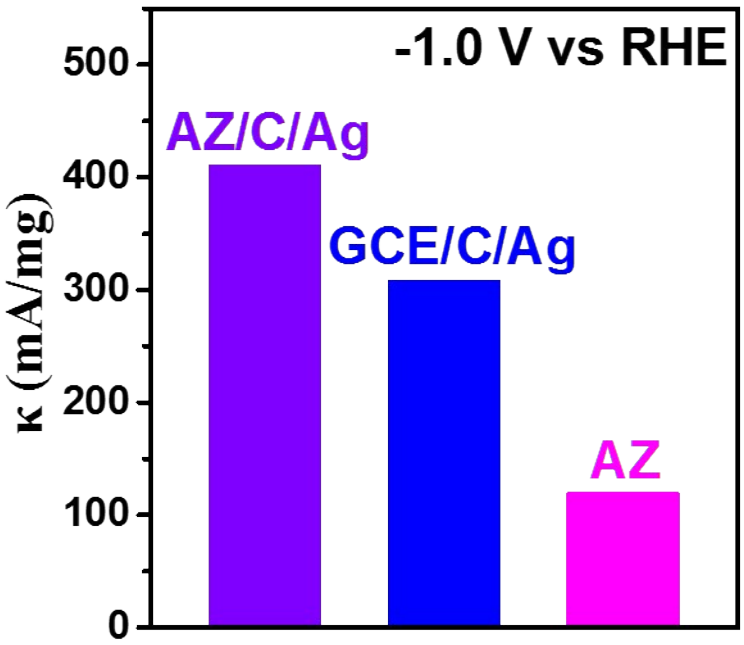

Figure S14. Mass activity for AZ, AZ/CB/Ag and GCE/C/Ag. Mass activity is based on the over mass of active AZ and Ag. Due to the low activity of Zn foil, the surface Zn nanoplates are mainly active components for CO_2RR, whose powder is measured to 3ug (0.2 mg/ 15 cm^{-2}).

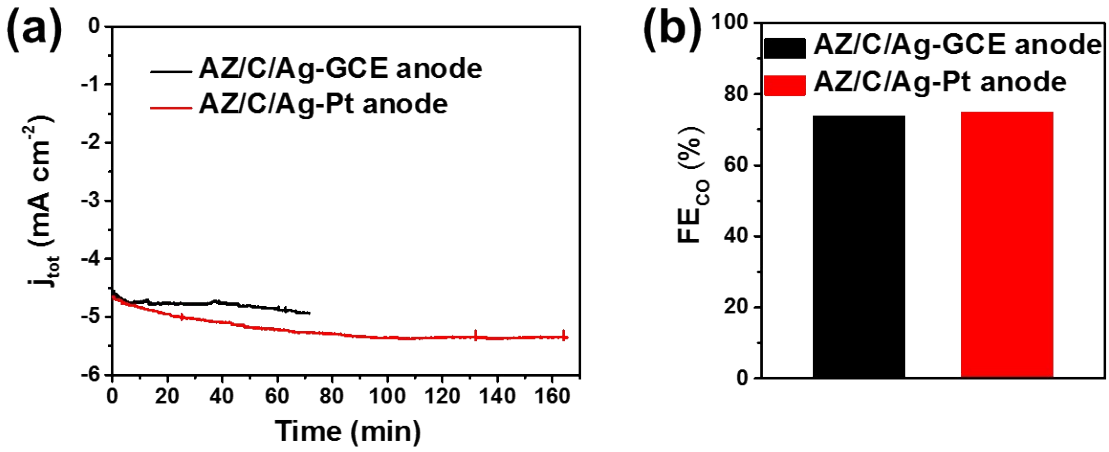

Figure S15 (a) Long term stabilities at a potential of -0.9V (b) the corresponding FEs of CO for AZ/C/Ag with GCE anode and Pt anode, respectively.

S6. A brief techno-economic analysis

We roughly estimated the cost of additional electrical energy consumed for preparing the anodized Zn electrode and the cost of Ag as follows.

In our work, the anodized Zn electrode (2 cm × 8 cm) were prepared at 30 V for 1 hour, the current during the preparation is kept at 10 mA. Thus, the electrical energy consumed during the preparation of anodized Zn can be calculated following the equation: W=UIt=30 V × 0.01 A × 1 h = 0.3 Wh. Assuming the electricity price is ~0.1445 dollar/kWh (the price is referring to the industrial electricity in China), the cost of electrical energy consumed to prepare the anodized Zn electrode is estimated to be 0.27×10^{-3} cent/cm^2.

The price of Ag according to the international trade price is ~0.5 dollar/g. To prepare the AZ/C/Ag electrode containing only 0.5 wt% Ag with electrode area of 0.22 cm^2, the amount of Ag used to fabricate the electrode is 1.5 μg. Therefore, the cost of Ag to fabricate AZ/C/Ag electrode containing only 0.5 wt% Ag is estimated to be: 0.34×10^{-3} cent/cm^2. That means even the Ag content in the electrode is as low as 0.5 wt%, the cost of Ag is even higher than that of the electrical energy consumed for preparing anodized Zn electrode. Considering most of the reported Ag containing electrodes usually contain more than 10 wt% Ag. The cost of Ag to fabricate these electrodes (containing 10 wt% Ag) should be 0.68×10^{-2} cent/cm^2, which is ~25 times higher than the cost of electrical energy consumed to preparing anodized Zn electrode. Although the selectivity and activity of the as-prepared AZ/C/Ag electrode is still slightly lower than the Ag containing electrode, the cost of our electrode could be greatly reduced. Additionally, the as-prepared AZ/C/Ag electrode exhibit relatively good stability during electrocatalytic CO_2 reduction reaction, and it is easy to

fabricate electrode with larger size. Thus, we believe that the as-prepared AZ/C/Ag electrode reported in our work could be possibly used in practical applications.

S7. Role of the carbon amount in the AZ/C/Ag electrodes

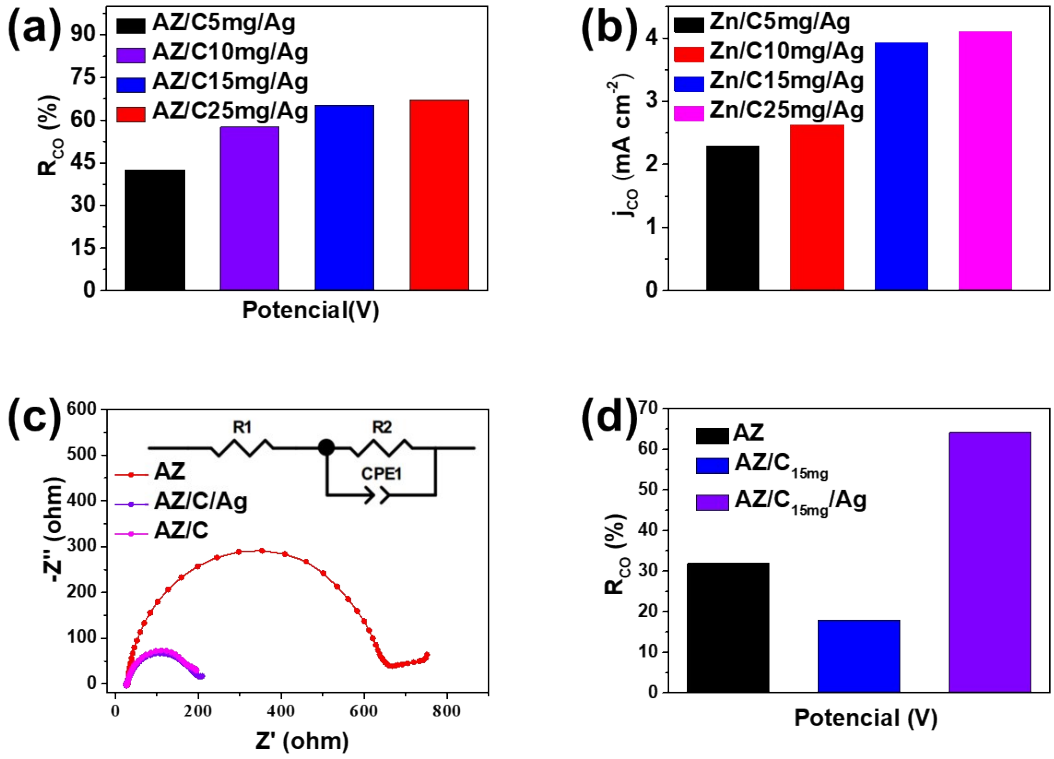

Figure S16. (a) Selectivity R_{CO} for the AZ/C/Ag electrode at a fixed potential with different amount of C. (b) Current density j_{CO} for the AZ/C/Ag electrode at fixed potential with different amount of C. (c) Electrochemical impedance spectra of the AZ, AZ/C and AZ/C/Ag electrodes. (d) R_{CO} of the AZ/C/Ag electrode and AZ/C electrode with 15 mg C.

S8. Computational section

1. Substrate models

To construct the model substrates for the AZ, GCE/C/Ag and AZ/C/Ag electrodes, we represent the AZ by four layers of Zn(111) (**Fig. S17a**), the C by two layers of diamond C(111) (**Fig. S17b**), and the Ag NPs by four layers of Ag(111) (**Fig. S17c**). In the rhombohedral unit cell of these three slabs, each Zn(111) layer has four Zn atoms, each Ag(111) layer has four Ag atoms, and each C(111) layer eight C atoms. Therefore, the Zn, C and Ag slabs each have 16 atoms per unit cell. Given that the C and Ag NP mixture of our experiments has only 1.8 wt% of Ag, the C slab consisting of only two C(111) layers. The side views of the substrates representing the three electrodes are given in **Fig. S17d**. For each of the Zn slab (**Fig. S17a**), C slab (**Fig. S17b**) and the Ag slab (**Fig. S17a**), we optimize the structure by DFT calculations after adding the vacuum layer of 36 Å and using a set of 9×9×1 k-points. The average cell parameters of the three slabs are calculated to be a = b = 5.35 Å. We use these average cell parameters to construct the three substrate structures for the three electrodes (**Fig. S17d**) and optimized their structures. We find that the distance between adjacent Zn(111) layers is 2.3 Å for the AZ substrate, and 2.4 Å for the AZ/C/Ag substrate. The distance between adjacent Ag(111) layers is 2.8 Å for the GCE/C/Ag substrate, and 2.6 Å for the AZ/C/Ag substrate. The distance between the C(111) and the adjacent Ag(111) is 3.4 Å in the GCE/C/Ag substrate, and 3.12 Å in the AZ/C/Ag substrate. The distance between the Zn(111) and the adjacent C(111) is 3.1 Å.

To obtain the adsorption energies of CO_2 on the surface of the AZ, GCE/C/Ag and AZ/C/Ag electrodes, we carried out geometry relaxations of the model substrates with CO_2 on the surface. The side and top views for the substrate plus CO_2 and COOH* are presented in **Fig. S18a - d**, respectively. The adsorption of CO_2 on the Ag surface increase the spacing between the adjacent C

layers in the GCE/C/Ag substrate (**Fig. 18Sa** and **18Sc**), but hardly changes the the spacing between the adjacent C layers in the AZ/C/Ag substrate (**Fig. 18Sa** and **18Sc**). In CO_2 adsorption, the Ag slab becomes strongly distorted from the layered structure (**Fig. 18Sa** and **18Sc**).

The adsorption energies calculated for CO_2, defined as

$\Delta E = E(\text{substrate + adsorbent}) - E(\text{substrate}) - E(\text{adsorbent})$

is summarized in **Fig. 5** in the text.

2. Computational details

The first-principles calculations were adopted on the basis of density functional theory (DFT) as implemented in the Vienna Ab Initio Simulation Package (VASP).[5,6] The electron exchange correlation was treated with the Perdew–Burke–Ernzerhof (PBE) in the framework of generalized gradient approximation (GGA).[7] The DFT Kohn-Sham equations were resolved by the projector augmented wave (PAW) through the plane wave basis set. The cutoff energy of 500 eV was chosen for plane-wave expansion of wave functions and Monkhorst–Pack (MP) scheme for k-point sampling was employed for the integration over the first Brillouin zone.[8] The 9×9×1 k-point mesh was used for the absorption structures. They were relaxed until the atomic forces on each ionic were less than 0.01 eV/Å-1 and the electron relaxation convergence criterion was 10-4 eV in two consecutive loops. In order to mimic the isolated layers, a vacuum space was set to 30 Å.

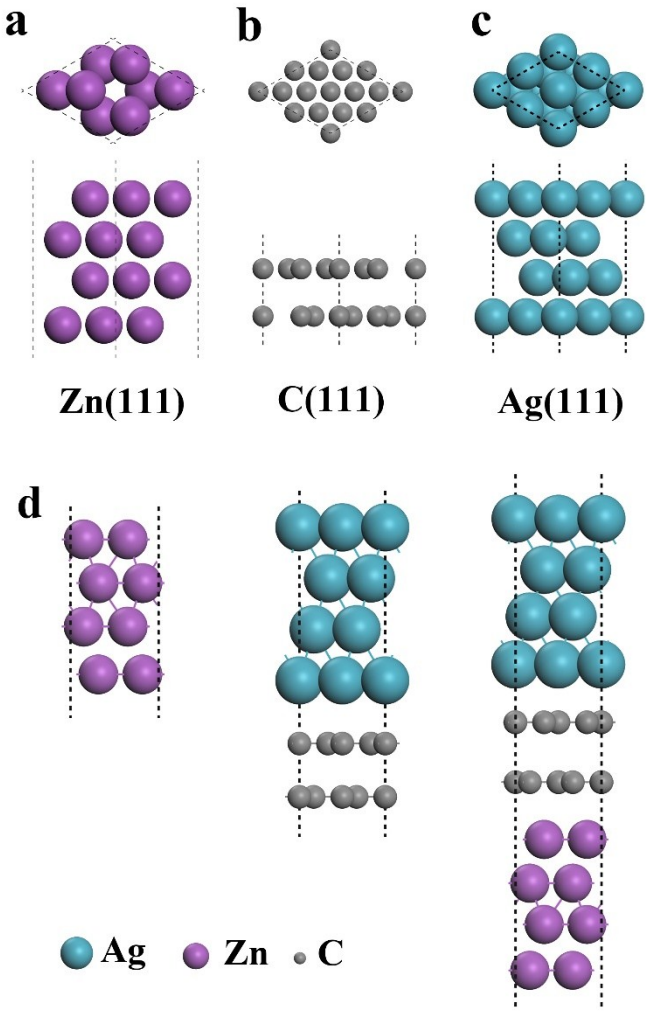

Figure S17. (a, b, c) Model substrates for the AZ, GCE/C/Ag and AZ/C/Ag electrodes, (d) side views of the substrates.

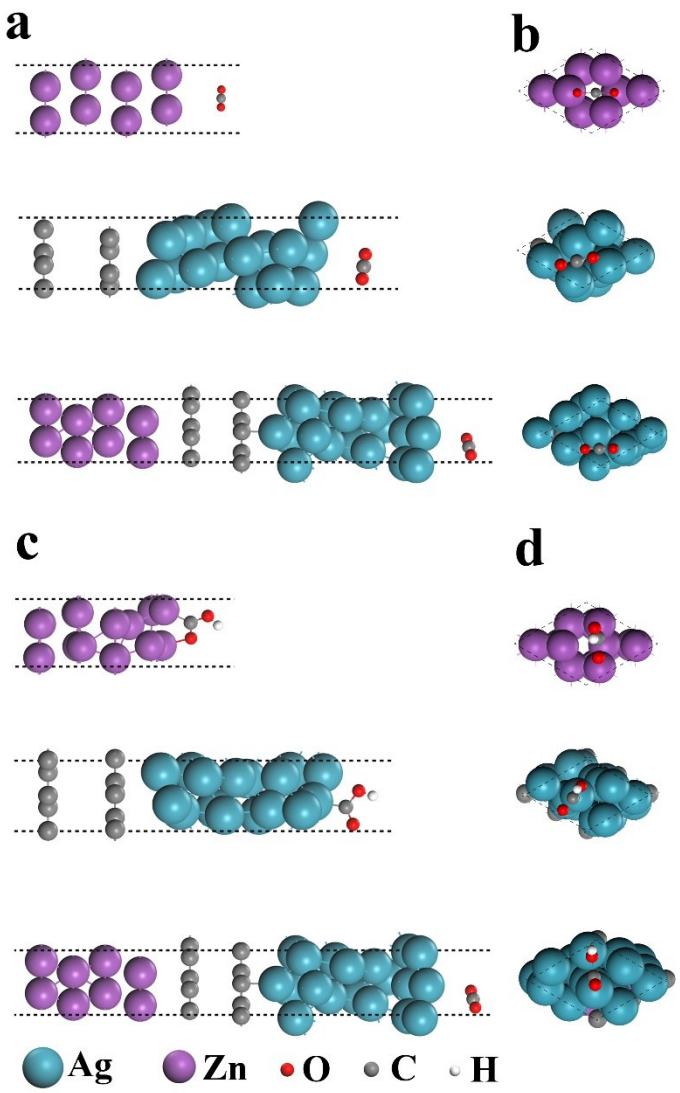

Figure S18. (a, b) Side and top views for the substrates plus CO_2 and COOH.

S9. Comparison of the mass activities of various CO_2RR catalysts

Sample	Ag amount (mg/cm^2)	electrolyte	j_{CO} (mA/cm^2)	FE_{CO} (%)	mass activity κ_{CO} (mA/mg_{cat})	Stability (h)	Ref
AZ/C/ Ag NPs	0.007	0.5M $KHCO_3/CO_2$	7.9	85.8	411	5	this work
GCE/C/ 5nm Ag	0.09	0.5M $KHCO_3/CO_2$	8.2	84.4	70	N/A	9
Porous Ag	~40	0.5M $KHCO_3/CO_2$	20	~90.0	0.5	2	10
GCE/C/ Tri-Ag	0.637	0.1M $KHCO_3/CO_2$	2	96.8	3	14	1
Ag NPs	6.7	EMIN-BF_4	~0.61	96	0.091	N/A	11
2nm Ag/Zn plates	N/A	0.1M $KHCO_3/CO_2$	1.89	84	~1.85	2	12
GCE/C/ gold-iron	0.25	0.5M $KHCO_3/CO_2$	35	97	140	90	13
Au nanowire	40.8	0.5M $KHCO_3/CO_2$	N/A	94	6.3	1	14

S8. References

1 Liu, S.; Tao, H.; Zeng, L.; Liu, Q.; Xu, Z.; Liu, Q.; Luo, J. L. *J Am Chem Soc* 2017, *139* (6), 2160-2163.

2 Y. Liang, Y. Li, H. Wang, J. Zhou, J. Wang, T. Regier and H. Dai, Nat Mater, 2011, 10, 780-786.

3 Y. Li, W. Zhou, H. Wang, L. Xie, Y. Liang, F. Wei, J. C. Idrobo, S. J. Pennycook and H. Dai, Nat Nanotechnol, 2012, 7, 394-400.

4 Won, D. H.; Shin, H.; Koh, J.; Chung, J.; Lee, H. S.; Kim, H.; Woo, S. I. *Angew. Chem. Int. Ed.* 2016, *55*, 9297-9300.

5 Kresse, G.; Joubert, D. Phys. Rev. B 1999, 59, 1758–1774.

6 Kresse, G.; Furthmuller, J. Phys. Rev. B: Condens. Matter Mater. Phys. 1996, 54, 11169.

7 Perdew, J. P.; Burke, K.; Ernzerhof, M. Phys. Rev. Lett. 1996, 77, 3865–3868.

8 Monkhorst, H. J.; Pack, J. D. Phys. Rev. B 1976, 13, 5188–5192.

9 Kim, C.; Jeon, H. S.; Eom, T.; Jee, M. S.; Kim, H.; Friend, C. M.; Min, B. K.; Hwang, Y. J. *J Am Chem Soc* **2015,** *137* (43), 13844-50.

10 Lu, Q.; Rosen, J.; Zhou, Y.; Hutchings, G. S.; Kimmel, Y. C.; Chen, J. G.; Jiao, F. *Nat Commun.* **2014,** *5*, 3242.

11 Rosen, B. A.; Salehi-Khojin, A; Thorson, M. R.; Zhu, W.; Whipple, D. T.; Kenis, P. J. A.; Masel, R. I. *science* **2011,** *334*, 643-644.

12 Q. Yu, X. Meng, L. Shi, H. Liu and J. Ye, Chem Commun (Camb), 2016, 52, 14105-14108.

13 Sun, K.; Cheng, T.; Wu, L; Hu, Y.; Zhou, J.; Maclennan, A.; Jiang, Z.; Gao, Y.; Goddard, W. A.; Wang, Z. *J. Am. Chem. Soc*. **2017**, *139*, 15608-15611.

14 Zhu, W.; Zhang, Y. -J.; Zhang, H.; Lv, H.; Li, Q.; Michalsky, R.; Peterson, A. A.; Sun, S. *J Am Chem Soc* **2014,** *136* (46), 16132-5.